Silicon (2017) 9:85–96
DOI 10.1007/s12633-014-9187-1

ORIGINAL PAPER

Oligosiloxanes with Silatrane Moieties for Use in Lithium-ion Conductive Matrices

Tomonobu Mizumo · Makoto Nakashima · Joji Ohshita

Received: 18 July 2013 / Accepted: 22 January 2014 / Published online: 21 November 2014

Abstract Solvent-free polymer electrolytes are critical for improving the performance of electrochemical devices. With the aim of developing a new silicon-based polymer electrolyte that does not contain poly(ethylene oxide) or ionic-liquid moieties, we present the synthesis, spectroscopic, thermogravimetric, and electrochemical characterization of a polymer combining flexible polysiloxanes with polar silatrane moieties at their chain ends or at their pendant chain ends prepared via hydrosilylation. The polymers obtained readily dissolve lithium bis (trifluoromethylsulfonyl)amide (LiTFSA), whereas lithium trifluoromethylsulfonate (LiOTf) and lithium bis(oxalato) borate (LiBOB) exhibit lower solubility. The polysiloxane with silatrane chain ends show an ionic conductivity of about 10^{-6} S cm^{-1} at ambient temperature, a wide electrochemical stability of 5.4 V, a high lithium-ion transference number of 0.70, and good long-time thermal stability up to 150 °C. The pendant-type polymers show lower ionic conductivity because of their high glass transition temperature. Despite their low conductivity, the solvent-free polymer/LiTFSA complexes might find application as binder materials.

Keywords Silatrane · Polysiloxane · Polymer electrolyte · Hydrosilylation

T. Mizumo (✉) · M. Nakashima · J. Ohshita
Department of Applied Chemistry,
Graduate School of Engineering, Hiroshima University,
Kagamiyama 1-4-1, Higashi-Hiroshima,
Hiroshima, 739-8527, Japan
e-mail: t.mizumo@eamex.co.jp

T. Mizumo
Eamex Corporation, Minatojima-Minamimachi 5-5-2,
Kobe, 650-0047, Japan

1 Introduction

Solvent-free electrolytes are important for the development of electrochemical power sources such as secondary batteries, fuel cells, and super capacitors. Among solvent-free systems, lithium-ion conductors have been extensively developed using both inorganic and organic materials, including ceramics, glasses, polymers, and ionic liquids [1–5]. Some of the newest materials possess high ionic conductivity, wide electrochemical window, high lithium-ion transference number, and thermal stability required for devices.

In the development of these electrolyte materials, silicon has played an important role. In particular, in polymer systems, polydimethylsiloxane (PDMS) has often been employed to provide conductive matrix with a low glass transition temperature (T_g). Specifically, poly(ethylene oxide) (PEO)-based polymer electrolytes bound to PDMS backbones show high ionic conductivity because of the low T_g [6–9]. For instance, oligo(dimethyl siloxane)s [5, 10] and hyperbranched polysiloxanes [11], on which oligo(ethylene oxide) chains were anchored, attain excellent ionic conductivities exceeding 10^{-3} S cm^{-1}.

However, polymer electrolytes with the PEO structure have some drawbacks such as low lithium-ion transference number [12] and relatively low thermal stability [13]. Therefore, polysiloxane-based non-PEO-electrolytes have also been suggested. The first such non-PEO-type polymer was a polysiloxane containing cyclic carbonate moieties prepared via hydrosilylation [14] and showed a high dielectric constant, thus dissolving a large amount of lithium trifluoromethylsulfonate (LiOTf), and an ionic conductivity of 10^{-7} S cm^{-1} at ambient temperature. A cross-linked polysiloxane with cyanide side chains was synthesized [15], and the conductivity of the $LiClO_4$-doped system exceeded

10^{-5} S cm^{-1}. More recently, oligosiloxanes on which cyclic carbonates are anchored were developed [16, 17] and utilized as polar additive for PEO-based materials. Furthermore, a lithium single-ion conductive polysiloxane, having a cyclic carbonate moiety and a lithium borate moiety as pendant units, was reported [18].

On the other hand, to date, few organosilicon compounds were utilized as the polar unit inducing salt dissociation. As a new organosilicon-based lithium-ion conductor, we have reported a silatrane/lithium-salt complex [19]. Silatranes are atranes with a pentacoordinated silicon center. Since the first report [20], the chemical properties, biological activity, and applications of silatrane derivatives have been studied [21–25]. Our previous study focused on the dissolution of lithium salt into the silatrane matrix, because silatrane was reported to possess a large dipole moment along the transannular dative bond [22]. As expected, silatranes dissolved several lithium salts such as LiOTf and lithium bis(trifluoromethylsulfonyl)amide (LiTFSA) to form amorphous silatrane/lithium-salt complexes. The complexes obtained showed moderate ionic conductivity of about 10^{-5} S cm^{-1} at ambient temperature, comparable to that of PEO systems [26]. Furthermore, the volatility of the complexes was low, and the decomposition temperatures exceeded 300 °C. These properties indicate that silatrane/lithium-salt complexes can be treated as quasi-solvent-free electrolytes.

Based on this result, we further examined a non-PEO-type polymer electrolyte composed of silatrane units. At first, methacryloylpropylsilatrane (MPS) was polymerized by the free-radical method [27]. However, the polyMPS/lithium-salt complexes showed no detectable ionic conductivity ($< 10^{-9}$ S cm^{-1}) caused by the high T_g of the polymer matrix exceeding 70 °C, resulting in insufficient free volume for ion migration. Accordingly, we herein present the synthesis of a new non-PEO-type polymer electrolyte having a low T_g by combining flexible polysiloxane and polar silatrane moieties. We describe the complex formability of this electrolyte with lithium salts, as well as its electrochemical properties (including ionic conductivity, electrochemical window, and lithium ion transference number) and thermal stability.

2 Experimental

2.1 Materials

Allyltriethoxysilane (TCI), 2,2',2''-nitrilotriethanol (triethanolamine, Nacalai Tesque), and polysiloxanes having hydrosilane moieties, including α, ω-dihydro poly (dimethylsiloxane) (PDMS-2H, Gelest, M_w = 1000–1100),1,3,5,7-tetramethylcyclotetrasiloxane (D_4H, Gelest), and poly(dimethylsiloxane-*co*-methylhydrosiloxane) (PDMS-*co*-PMHS, trimethylsiloxy-terminated, M_w = 1900–2000, content of the methylhydrosiloxane units = 25–30 mol%, Gelest) were used as received. The specific number-average molecular weight (M_n) of PDMS-2H was determined by proton nuclear magnetic resonance (^{1}H NMR) spectroscopy as 735. Because M_n of PDMS-*co*-PMHS was difficult to determine by ^{1}H-NMR, the values supplied by Gelest were employed. Chloroplatinic acid hexahydrate (Nacalai Tesque) was used after preparing a 0.1 mol L^{-1} solution of anhydrous isopropanol. Lithium salts including LiOTf (Kanto Chemical), LiTFSA (Kanto Chemical), and lithium bis(oxalato)borate (LiBOB, Kishida Chemical) were stored and treated in a stainless-steel glove box (UN-650F, UNICO) filled with argon gas. Toluene (Wako Pure Chemical) was first dried on a column with activated alumina (basic, 200-mesh, Nacalai Tesque) under argon and subsequently over a molecular sieve 4A. Acetonitrile (HPLC grade, Wako Pure Chemical) was dried over molecular sieve 4A. Activated alumina for the purification of the synthesized oligomers (Merck, neutral, with 90 Å mean pore size) and polystyrene beads for gel permeation chromatography (S-X3, Biorad) were used as received. Eleven other solvents and reagents were purchased from Wako Pure Chemical and used as received.

2.2 Preparation of Allylsilatrane

A mixture of allyltriethoxysilane (8.88 g, 0.044 mol), triethanolamine (5.97 g, 0.040 mol), and potassium hydroxide (13 mg) in toluene (45 mL) was heated to 100 °C for 3 h while the generated ethanol was removed by distillation, as confirmed by gas chromatography via the disappearance of triethanolamine. After the reaction mixture was concentrated by rotary evaporation, a crude product was precipitated using hexane (200 mL). The precipitate was extracted with 150 mL of toluene, and the organic phase was washed thrice with brine (10 mL) and then dried over anhydrous magnesium sulfate. After filtration, the solvent was removed under vacuum, and the residue was recrystallized from a mixture of hexane (50 mL) and a small amount of toluene to obtain a white acicular crystal (6.74 g, 78 % yield):

mp 120 °C; ^{1}H NMR (CD_3OD): δ = 1.29 (dt, 1.2 Hz, 2H, $C\underline{H}_2Si$), 2.87 (t, 6H, $C\underline{H}_2N$), 3.72 (t, 6H, $SiOC\underline{H}_2$), 4.60–4.75 (m, 2H, $C\underline{H}_2$ =CH), 5.86 (m, 1H, CH_2 =C$\underline{H}$); ^{13}C NMR (CD_3OD): δ = 25.9 ($\underline{C}H_2Si$), 51.7 ($\underline{C}H_2N$), 58.5 ($SiO\underline{C}H_2$), 111.1 (CH_2 =$\underline{C}$H), 139.9 ($\underline{C}H_2$ =CH); GC/EI MS m/z = 215 (M^+), 174 (M^+ – CH_2CH = CH_2).

2.3 Preparation of α, ω-disiloxanylpropyl Poly(dimethylsiloxane) (PDMS-2SiA)

A solution of allylsilatrane (1.00 g, 4.7 mmol), PDMS-2H (1.69 g, 2.3 mmol) in toluene (8 mL) was added a 20 μL isopropanol solution of chloroplatinic acid hexahydrate at room temperature. The mixture was heated to 50°C for 10 h under stirring until Fourier transform infrared (FT-IR) spectroscopy confirmed the disappearance of the Si–H absorption band at 2127 cm^{-1}. After cooling, the reaction mixture was added to hexane (50 mL) to precipitate unreacted allylsilatrane. After filtering the solution through Celite, the solvent was removed from the filtrate under vacuum to obtain the crude product as a viscous liquid, which was further purified by column chromatography on neutral alumina with hexane/ ethylacetate = 5/ 3 (v/v) to obtain a colorless viscous liquid (1.85 g, 82 % yield):

^{1}H NMR ($CDCl_3$) $\delta = 0.02 - 0.12$ (m, $(CH_3)_2Si$), 0.49 (t, $CH_2Si(OC_2H_4)_3$), 0.61 (t, $OSi(CH_3)_2CH_2$), 1.42 (m, $CH_2CH_2CH_2$), 2.78 (t, CH_2N), 3.75 (t, $SiOCH_2$); ^{13}C NMR ($CDCl_3$): δ = 0.3 ($OSi(CH_3)_2CH_2$), 1.1 ($OSi(CH_3)_2O$), 18.6 ($CH_2CH_2CH_2$), 21.0 ($CH_2Si(OC_2H_4)_3$), 23.2 ($OSi(CH_3)_2CH_2$), 51.2 (CH_2N), 57.9 ($SiOCH_2$); ^{29}Si NMR ($CDCl_3$): δ = 7.61 ($OSi(CH_3)_2CH_2$), –21.87 ($OSi(CH_3)_2O$), –65.38 ($CH_2Si(OC_2H_4)_3$); FT-IR (neat): ν(Si-N) = 583 cm^{-1}, ν(Si-C) = 606 cm^{-1}, ρ(Si-CH_3) = 800 cm^{-1}, ν(C-N) = 905 cm^{-1}, ν_{as}(Si-O-Si) = 1024–1105 cm^{-1}; M_n = 1191 (estimated by ^{1}H NMR).

2.4 Preparation of 1,3,5,7-tetramethyl-1′,3′,5′,7′-tetrapropylsilatranyl cyclotetrasiloxane (D_4-SiA)

A solution of allylsilatrane (0.71 g, 3.3 mmol) and D_4H (1.20 g, 0.8 mmol) in toluene (1 mL) was added a 5 μL of isopropanol solution of chloroplatinic acid hexahydrate at room temperature. The mixture was heated to 70 °C for 24 h under stirring until the disappearance of the Si–H absorption band at 2173 cm^{-1} in the FT-IR spectra. The reaction mixture was added 30 mL of toluene and filtered through Celite. The solution was concentrated by rotary evaporation from which the product was isolated by preparative gel permeation chromatography eluted with toluene. Removing the solvent under vacuum yielded a colorless viscous liquid (0.51 g, 57 % yield).

^{1}H NMR ($CDCl_3$): δ = 0.01–0.14 (m, 12H, CH_3Si), 0.47 (m, 8H, $O_2Si(CH_3)CH_2$), 0.54–0.63 (m, 8H, $CH_2Si(OC_2H_4)_3$), 1.40–1.48 (m, 8H, $CH_2CH_2CH_2$), 2.69–2.78 (t, 24H, CH_2N), 3.65–3.75 (t, 24H, $SiOCH_2$); ^{13}C NMR ($CDCl_3$): δ = –0.5 (CH_3Si), 18.4 ($CH_2CH_2CH_2$), 20.6 ($CH_2Si(OC_2H_4)_3$), 22.0 ($O_2Si(CH_3)CH_2$), 51.2 (CH_2N), 58.0 ($SiOCH_2$); ^{29}Si NMR ($CDCl_3$): δ = –20.3 ($O_2Si(CH_3)CH_2$), –64.3 ($CH_2Si(OC_2H_4)_3$); ESI MS: m/z = 1124.4 [M + Na^+].

2.5 Preparation of Poly(dimethylsiloxane-*co*-methylpropyl silatranylsiloxane) (PDMS-*co*-PMSiAS)

A solution of allylsilatrane (0.67 g, 3.1 mmol) and PDMS-*co*-PMHS (0.56 g) in toluene (4 mL) was added a 5 μL isopropanol solution of chloroplatinic acid hexahydrate at room temperature and heated to 60 °C for 72 h under stirring, until the disappearance of the Si–H absorption band at 2150 cm^{-1} in the FT-IR spectrum. The reaction mixture was added 30 mL of chloroform and filtered with Celite and concentrated by rotary evaporation. The crude product was isolated by preparative gel permeation chromatography eluted with toluene. After removing the solvent under vacuum, a viscous liquid was obtained (0.83 g, 82 % yield). An M_n of 2536 was determined by ^{1}H-NMR, and the number of PDMS and PMSiAS units was 13.5 and 5, respectively.

^{1}H NMR ($CDCl_3$)δ = 0.04 (d, 18H, terminal TMS), 0.07 (m, 72H, CH_3Si-), 0.46 (br, 10H, $O_2Si(CH_3)CH_2$), 0.57 (br, 10H, $CH_2Si(OC_2H_4)_3$), 1.45 (br, 10H, -$CH_2CH_2CH_2$), 2.76 (br, 30H, CH_2N), 3.72 (br, 30H, $SiOCH_2$).

2.6 Preparation of Polymer/lithium-salt Complexes

Polymer and lithium salt were homogeneously dissolved in dry acetonitrile. The polymer/salt complex was obtained by drying in a vacuum oven (0.05 Torr, 50 °C for at least 24 h), until the disappearance of acetonitrile was confirmed by ^{1}H NMR.

2.7 Analytical Methods

^{1}H, ^{13}C, and ^{29}Si NMR spectroscopy were performed in $CDCl_3$ or CD_3OD solutions, and spectra were recorded on a VNMR S-500 spectrometer (Varian). The ^{29}Si NMR spectra were collected with a relaxation delay of 20.0 s. The thermal stability of the materials under N_2 gas was examined by thermogravimetric analysis (TGA) performed using an Exstar TG/DTA6200 (Seiko Instruments Inc.). The samples (5–10 mg) were loaded in aluminum pans and heated from ambient temperature to 500 °C, at a rate of 10 K min^{-1}, under a N_2 flow rate of 250 mL min^{-1}. Differential scanning calorimetry (DSC) was performed on an Exstar DSC 6200 (Seiko Instruments Inc.). Samples (5–10 mg) were placed in a sealed aluminum pan and heated from −120 to 200 °C at a rate of 10 K min^{-1}. FT-IR spectroscopy was performed on an IRAffinity-1 FTIR spectrometer (Shimadzu) by recording the transmis-

sion spectra in the range 4000–400 cm^{-1}. Samples for analysis were sandwiched between a pair of KBr plates. Electron spray ionization mass spectrometry (ESI MS) was performed on an ESI 4000Q-TRAP mass spectrometer (AB Sciex) by injecting the sample solution (100–200 ng mL^{-1} in acetonitrile) directly into the ion source. The bulk ionic conductivity was determined by complex impedance spectroscopy using a Solatron-1260 frequency response analyzer (Solatron Analytical). The samples were sandwiched between a pair of stainless steel discs (SUS-316L, 15.5 mm in diameter) with a poly(ethylene terephthalate) spacer (area: 0.237 cm^2; thickness: 250 μm) and loaded into a sealable two-electrode electrochemical cell (HS-Cell, Hohsen). The cell was assembled in a glove box (UNICO 650L) filled with argon. The temperature of the cell was controlled by a VTH-1000 Peltier controller (VICS). Measurements were performed at frequencies ranging from 1 MHz to 100 Hz with an oscillating voltage of 100 mV. The elemental values of Voigt-type equivalent circuits were determined by the nonlinear least squares fitting method using the Scribner Associates Z-view. The ionic conductivities (σ_i) of the samples were obtained from the bulk resistance (R_b) according to the relation $\sigma_i = \kappa/R_b$, where κ is the cell constant determined using aqueous 0.01M KCl. The apparent lithium-ion transference numbers (t_{Li}^{+}) were determined by a combination of complex impedance spectroscopy and dc polarization with a dc bias of 10 mV [28], performed with an electrochemical analyzer VersaSTAT-4 (Princeton Applied Research). The measurement was carried out at 80 °C using the HS-Cell in which samples were sandwiched between a pair of lithium-foil discs (15.5 mm in diameter, 250 μm thick, Honjo Chemical; SUS-316L discs were employed as supporter/current corrector) with a polypropylene (PP) spacer (area: 0.237 cm^2; thickness: 200 μm). The electrochemical stability was investigated by cyclic voltammetry (CV) at a sweep rate of 5 mV s^{-1} at 80 °C using the HS-Cell consisting of a SUS-316L disc as the working electrode, a lithium-foil disc as the reference/counter electrode, and a PP spacer.

3 Results and Discussion

3.1 Syntheses and Characterizations

A series of polysiloxanes carrying silatrane moieties were prepared by hydrosilylation between allylsilatrane and the corresponding polysiloxane having hydrosilane groups (Scheme 1). In the presence of chloroplatinic acid (Speier's catalyst), the hydrosilylations proceeded under mild conditions.

The obtained PDMS-2SiA, D_4-SiA, and PDMS-*co*-PMSiAS were viscous fluids. DSC curves of the polymers displayed no melting points (T_m), implying that these polymers are amorphous (Fig. 1). The T_g values of PDMS-2SiA, D_4-SiA, and PDMS-*co*-PMSiAS were –73, 37, and –31 °C, respectively.

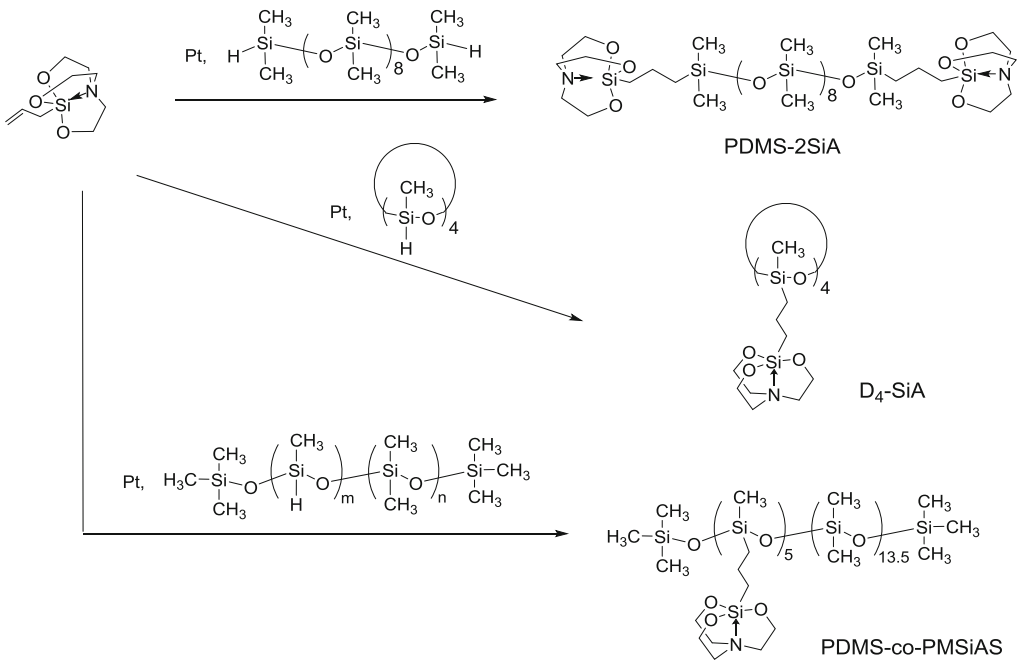

Scheme 1

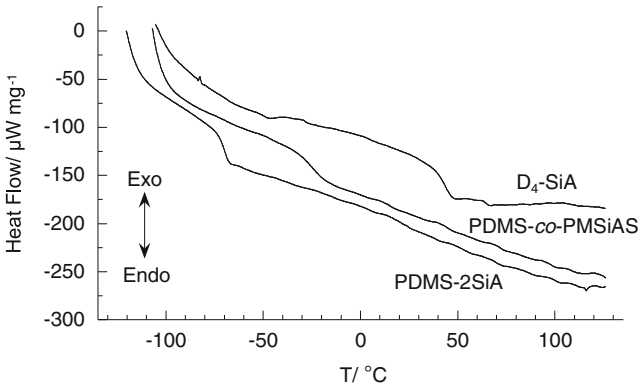

Fig. 1 DSC curves for pure PDMS-2SiA, D_4-SiA, and PDMS-co-PMSiAS

The polymers were spectroscopically characterized by ^{1}H, ^{13}C, and ^{29}Si NMR spectroscopy, and FT-IR spectroscopy. The spectra for PDMS-2SiA are shown in the Figs. 2 and 3. The ^{1}H NMR spectrum confirmed the disappearance of the allyl and hydrosilyl peaks at 4.8 and 5.9 ppm and at 4.6 ppm, respectively. The peaks assignable to the PDMS moiety (^{1}H: 0.06 ppm; ^{13}C: 0.4–1.2 ppm; ^{29}Si: –21.9 ppm), the silatrane moiety (^{1}H: 2.8 and 3.7 ppm; ^{13}C: 51.2 and 57.9 ppm; ^{29}Si: –65.4 ppm), and the propylene-bridge (^{1}H: 0.5, 0.6 and 1.4 ppm; ^{13}C: 18.6, 21.0 and 23.2 ppm; ^{29}Si: 7.6 ppm), respectively, were clearly found. The small peaks at 0.9–1.2 ppm (^{1}H NMR) indicate that small amounts of α-addition compounds coexist in the system.

The assignment of the FT-IR bands was performed according to a literature procedure [29–31]. The characteristic absorption peaks of the allyl group (1630 cm^{-1}) and hydrosilyl group (2127cm^{-1}) disappeared, whereas the characteristic absorption bands of PDMS, propylene-bridge, and the silatrane moieties emerged (Fig. 3).

3.2 Complex Formation with Lithium Salts

Each silatrane-containing polymer was dissolved in acetonitrile with an appropriate amount of lithium salt: LiTFSA, LiOTf, or LiBOB. Removing acetonitrile from the solution under reduced pressure yielded a complex of the polymer and the lithium salt. The dissolution state of a series of salts

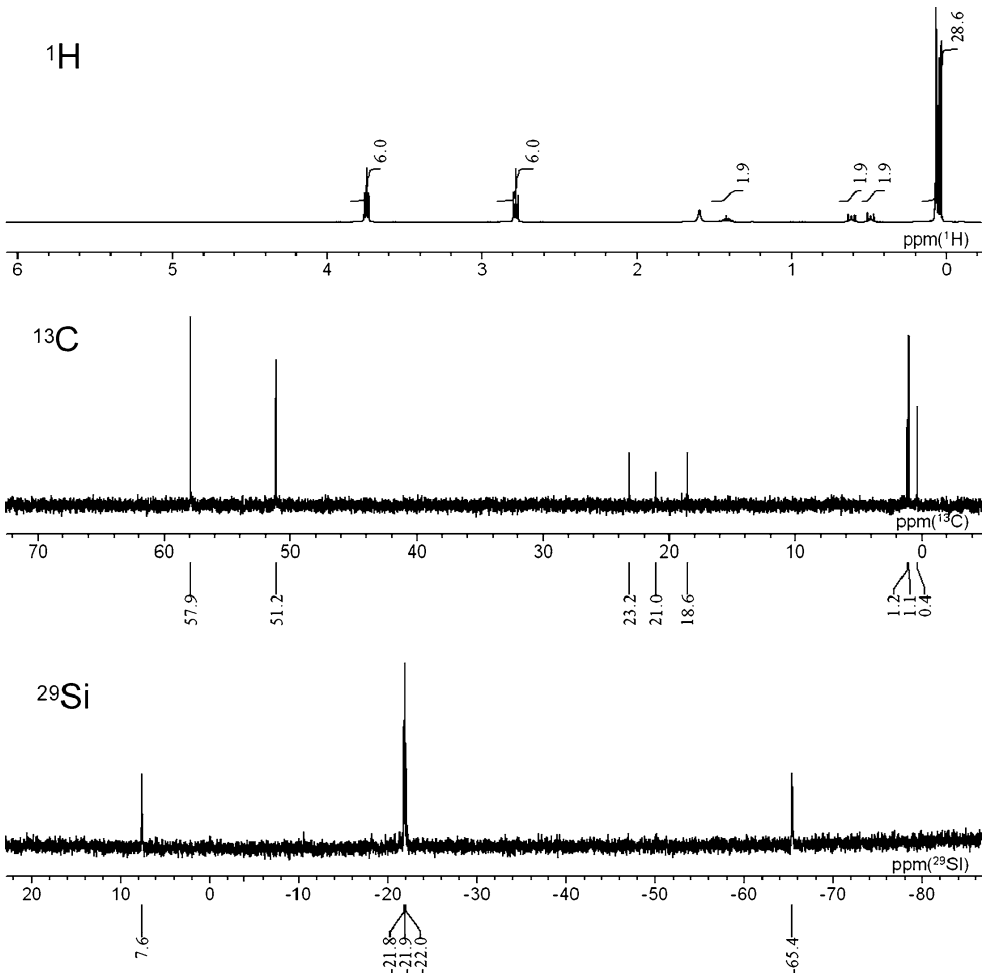

Fig. 2 ^{1}H, ^{13}C, and ^{29}Si NMR spectra of PDMS-2SiA

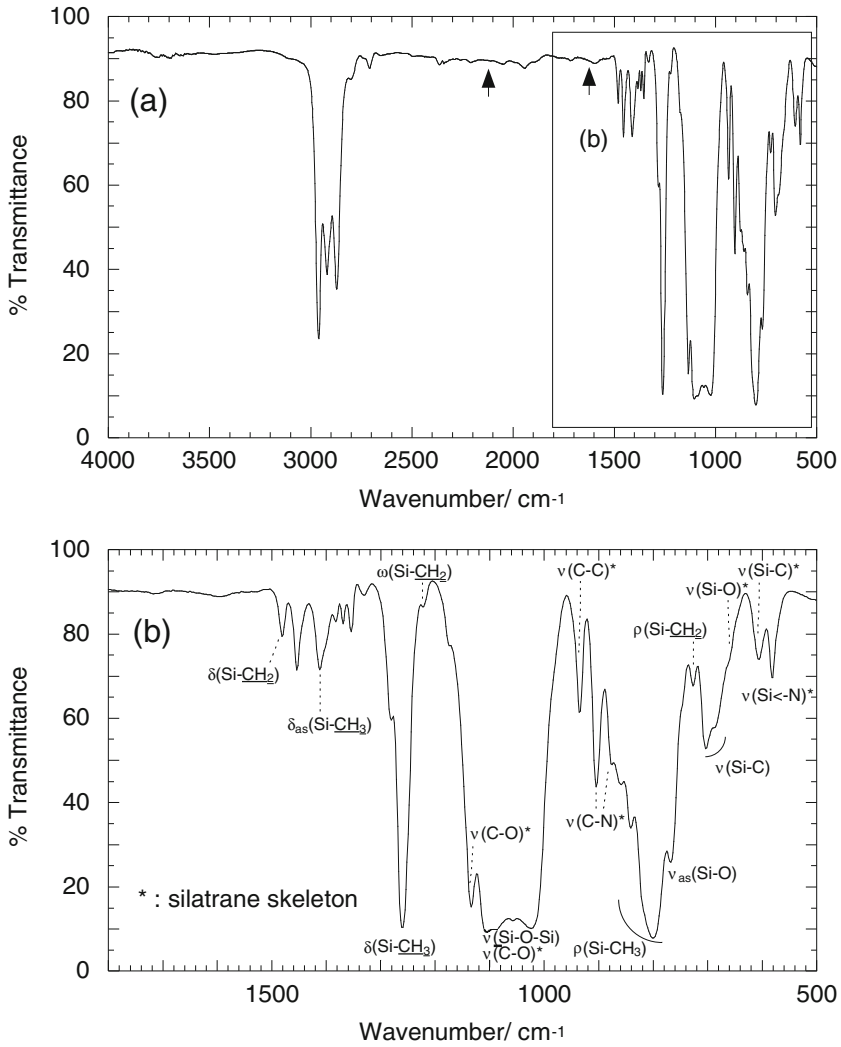

Fig. 3 FT-IR spectrum of PDMS-2SiA

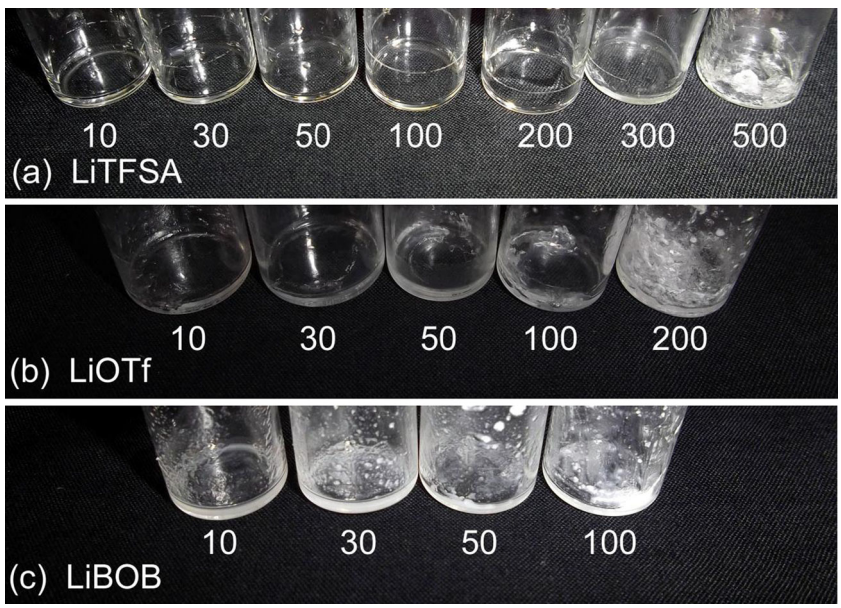

Fig. 4 Photographs of PDMS-2SiA/lithium-salt complexes containing **a** LiTFSA, **b** LiOTf, and **c** LiBOB at the mole percentage of the lithium salt with respect to the silatrane units (mol/mol) indicated by the numbers

in PDMS-2SiA is shown in the photographs of Fig. 4. The complexes containing LiTFSA were transparent viscous fluids up to salt concentrations of 200 mol% with respect to the silatrane moiety. At salt concentrations exceeding 300 mol%, the complex became a white-turbid solid characterized by a sharp endothermic peak at 150–160 °C on the DSC chart. These peaks were attributed to the melt of segregated LiTFSA itself [32].

The complexes with LiOTf were slightly turbid, viscous fluids until the salt concentration reached 100 mol%. On the DSC chart, these complexes showed an endothermic peak at around 60–70 °C (Table 1). Given that the melting point of pristine LiOTf is 423°C [32], these peaks may be attributable to the melting point of the crystalline LiOTf/polymer complex.

In the case of LiBOB, salt segregation already occurred at low concentrations. This low solubility of LiBOB in the polymer is an unexpected result because LiBOB is highly dissociative [33], and its estimated ion-pair binding energy is comparable to that of the other two salts (ca. 500 kJ mol^{-1}) [34, 35].

The LiTFSA and LiOTf complexes showed an increase in T_g with increasing salt concentration, whereas T_g of the LiBOB system remained constant (Fig. 5). The elevation of T_g in the LiTFSA and LiOTf systems indicates a strong interaction between ions and polar sites on the polymer chain, giving rise to ion solvation; however, it also induced the suppression of the segmental motion of the polymer [36].

On the other hand, the T_g of the LiTFSA system unexpectedly reached a plateau of about –35 °C at salt concentrations exceeding 50 mol%. The suppression in the T_g increase remains unresolved at present but it might be caused by the plasticization effect of LiTFSA [26, 37]. Similar plateaus and decreases in T_g at high LiTFSA concentrations were observed in D_4-SiA and PDMS-*co*-PMSiAS polymer matrices (Table 1).

3.3 Thermal Stability

The TGA chart for the PDMS-2SiA and its 50 mol% LiTFSA complex is shown in the Fig. 6a. Under general

Table 1 T_g, T_m and conductivity for a series of silatrane/lithium-salt complexes

Polymer	Salt	mol% salt/silatrane	T_g	T_m	σ_i(60°C) / S cm^{-1}[a]
PDMS-2SiA	–	0	–73	nd	-
	LiTFSA	10	–72	nd	4.6×10^{-6}
		30	–61	nd	11.5×10^{-6}
		50	–42	nd	17.7×10^{-6}
		100	–40	nd	6.0×10^{-6}
		200	–32	nd	2.1×10^{-6}
		300	–32	152	2.7×10^{-6}
		500	–39	160	1.9×10^{-6}
	LiOTf	10	–77	69	0.5×10^{-6}
		30	–77	67	0.8×10^{-6}
		50	–72	65	1.0×10^{-6}
		100	–47	58	–
	LiBOB	10	–79	nd	0.4×10^{-6}
		30	–79	nd	–
		50	–80	nd	0.5×10^{-6}
		100	–79	nd	–
D_4-SiA	–	0	37	nd	–
	LiTFSA	50	55	nd	64×10^{-9}
		100	21	nd	4.2×10^{-9}
	LiOTf	50	70	nd	nd
		100	80	nd	–
PDMS-*co*-PMSiAS	–	0	–31	nd	–
	LiTFSA	10	–23	nd	1.0×10^{-6}
		30	–12	nd	1.4×10^{-6}
		50	–5	nd	0.6×10^{-6}
		100	0	nd	0.9×10^{-6}

a: values at cooling scan; nd: not detected; –: not measured

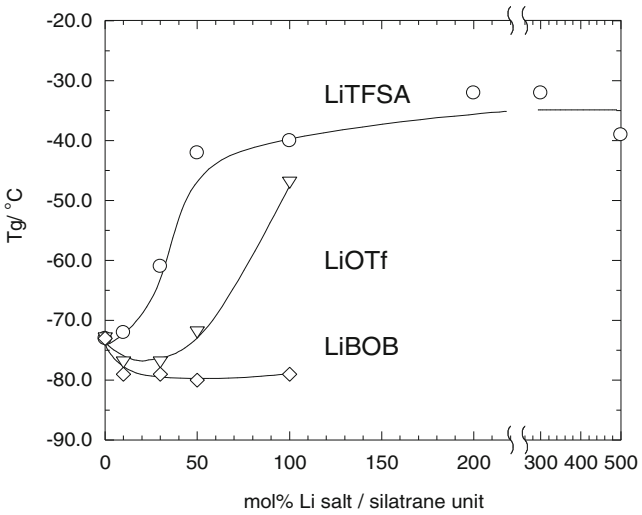

Fig. 5 Variation in glass transition temperature of PDMS-2SiA/lithium-salt complexes as a function of lithium-salt concentration, expressed as the mole percentage with respect to the number of silatrane units

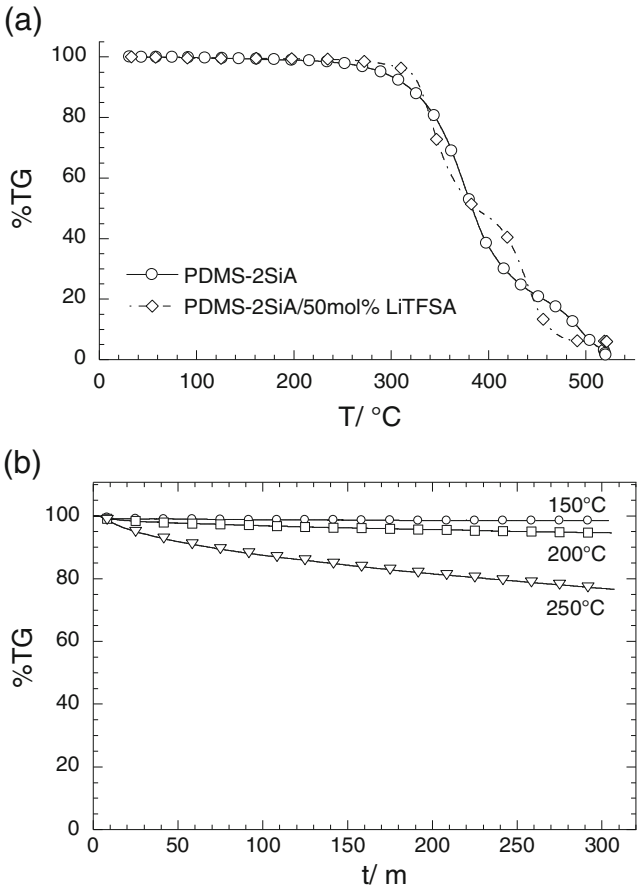

Fig. 6 Thermogravimetric charts for PDMS-2SiA measured under an N_2 atmosphere: **a** variation in sample weights in a heating ramp of 10 K min^{-1}, and **b** time dependence of sample weights for temperatures held at 150, 200, and 250 °C

analytical conditions, upon heating at 10 K min^{-1}, the polymer matrix began to decompose at around 320 °C, whereas LiTFSA decomposed at about 400 °C [32]. The observed decomposition temperature of 320 °C is superior to that of PEO (*ca.* 230 °C) [13] and comparable to that of ionic liquids [38, 39].

Long-time durability of PDMS-2SiA was further evaluated by maintaining the temperature at 150, 200, and 250 °C for 5h (Fig. 6b). The weight loss increased with increasing temperature from 0 over 4 to 20 % at 150, 200, and 250 °C. We therefore concluded that our polymer is adequately stable up to 150 °C.

3.4 Ionic Conductivity

The conductivities at 60 °C of polymers/lithium-salt complexes measured by the impedance spectroscopy are summarized in Table 1. Figure 7 displays the Arrhenius plot of the ionic conductivity for PDMS-2SiA doped with various LiTFSA contents. With increasing salt concentration, the number of carrier ions should increase, but the PDMS-2SiA/LiTFSA complexes also showed an increase in the apparent activation energy. Consequently, the optimum ionic conductivity was observed at a LiTFSA concentration of 50 mol% with respect to the number of silatrane units and reached 1.4×10^{-6}, 1.8×10^{-5} and 8.4×10^{-5} S cm^{-1} at 25, 60, and 100 °C, respectively. Additionally, the PDMS-2SiA/ 50 mol% LiTFSA complex yielded conductivities of 1.9×10^{-4}, and 3.4×10^{-4} S cm^{-1} at 150 °C and 200 °C, respectively.

Despite its higher T_g, the LiTFSA-doped systems showed higher conductivity than those containing LiOTf or LiBOB (Table 1), indicating that the LiTFSA can supply more carrier ions than other salts in the polymers investigated. The Vogel-Fulcher-Tammann (VFT) (1) was used to estimate the number and mobility of carrier ions (Table 2). The fitting parameters σ_0 and B relate to the number of carrier ions and the activation energy for ion mobility, respectively.

$$\sigma_i = \sigma_0 \, exp \frac{-B}{T - T_0} \tag{1}$$

As seen from Table 2, systems doped with LiTFSA and LiOTf exhibited the largest number of carrier ions and activation energy, respectively. The large activation energy for the PDMS-2SiA/LiOTf complex might arise from the crystalline phase, evidenced in the DSC results. Indeed, the Arrhenius plot of the conductivity for the LiOTf-doped systems showed branching points, close to the melting points observed in DSC (Fig. 8) between curves from heating and cooling scans.

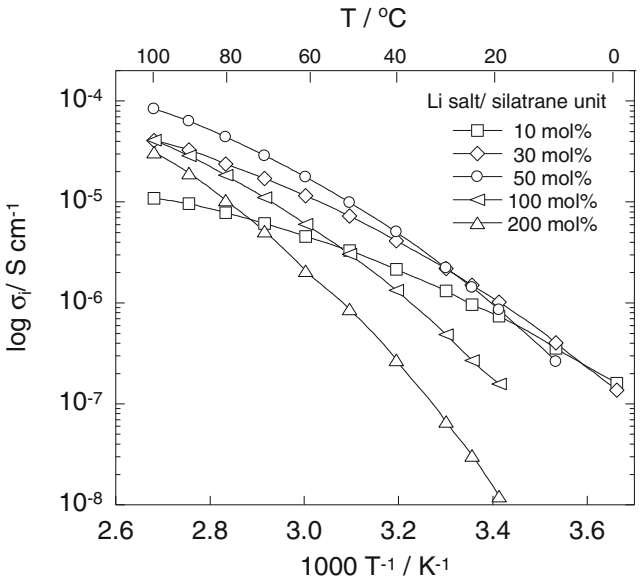

Fig. 7 Temperature dependences of the ionic conductivity for PDMS-2SiA/ LiTFSA complexes with various salt concentrations

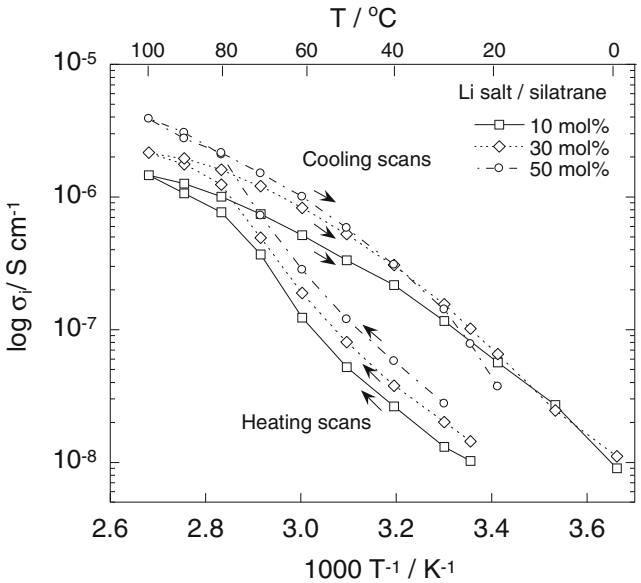

Fig. 8 Temperature dependences of the ionic conductivity of PDMS-2SiA/LiOTf complexes with various salt concentrations

The effect of polymer structure on ionic conductivity was also examined (Fig. 9 and Table 1). The ionic conductivity of D_4-SiA and PDMS-*co*-PMSiAS was lower than that of PDMS-2SiA by several orders of magnitude and likely caused by their high T_g, which was also observed in our previous study on poly(methacryloylsilatrane)s [19]. The high T_g of these polymers is presumably due to their comb structure with silatrane moieties on the pendant ends, allowing for multi-point dipole-dipole interactions between silatrane moieties as well as dipole-ion interactions between silatrane moiety and ionic species. Although we expected the comb-type polymers to provide carriers owing to their larger polarity, the strong ion-polymer electrostatic interactions suppressed carrier transportation.

Figure 10 summarizes the relation between the conductivity and T_g for a series of polymer/lithium-salt complexes in the present study. When T_g exceeded –40 °C, the ionic conductivity decreased constantly for all polymers, whereas it increased for T_g below –40 °C, reaching its maximum of about 10^{-5} S cm^{-1} at $T_g = -40$ °C.

Table 2 VFT parameters for PDMS-2SiA doped with a variety of lithium salts at a salt concentration of 50 mol% with respect to the silatrane units

Salt	σ_0/ S cm^{-1}	B/ K	T_0/ K
LiTFSA	0.00471	581	229
LiOTf	0.00030	721	206
LiBOB	0.00005	693	186

3.5 Electrochemical Stability

To determine the potential window of the PDMS-2SiA/50 mol% LiTFSA complex, electrochemical measurements were carried out in a two-electrode cell with stainless steel SUS316L and lithium metal as working and reference/counter electrodes, respectively. The measurement was carried out at 80 °C to obtain an adequate current. The cyclic voltammogram, displayed in Fig. 11, clearly shows the deposition/stripping of lithium and the anodic

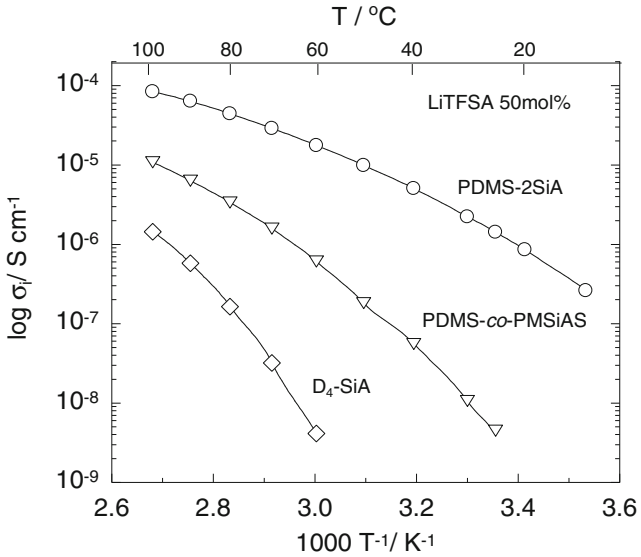

Fig. 9 Arrhenius plots of the ionic conductivity of polymer/LiTFSA complexes for various polymers at a salt concentration of 50 mol% with respect to the silatrane units

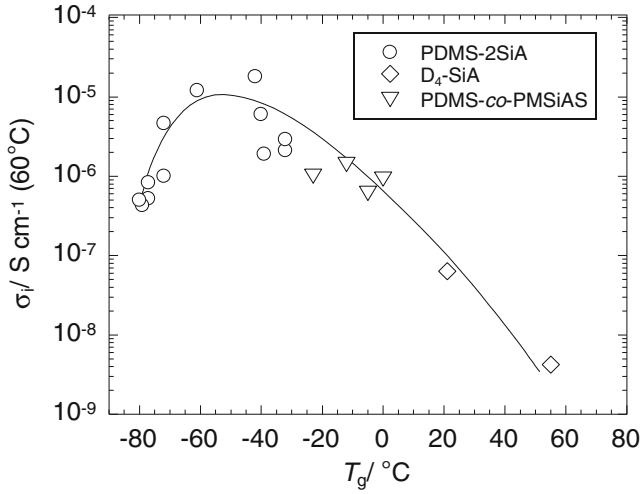

Fig. 10 Variation in the ionic conductivity at 60°C of a series of polymer/lithium-salt complexes as a function of the glass transition temperature

limit at 5.4 V with respect to the potential of Li^+/Li, indicating that this material has a wide potential window among polymer electrolytes [26, 38]

3.6 Lithium-ion Transference Number

The lithium-ion transference number of the PDMS-2SiA/50 mol% LiTFSA complex was determined from measurements in a two-electrode cell with a pair of lithium metal discs as working and reference/counter electrodes. The time dependence of the current at constant potential (10 mV) is shown in Fig. 12a. The initial current (I_i) 1.9 μA decayed to a steady-state current (I_s) of 1.3 μA after 10,000 s. Figure 12b shows the Nyquist plot after 40,000 s of polarization. The small interfacial resistance at the steady-state (Ri_s) 500 Ω, an increased from the initial interfacial resistance (Ri_i) of 220 Ω, indicates facile charge transfer between the lithium metal electrode and electrolyte. However, the resistance of the bulk electrolyte (Rb) increased from 5300 Ω to 7200 Ω during the polarization, suggesting reaction of the polymer with the lithium metal. The lithium-ion transference number (t_{Li+}) of 0.70 was obtained from Eq. 2:

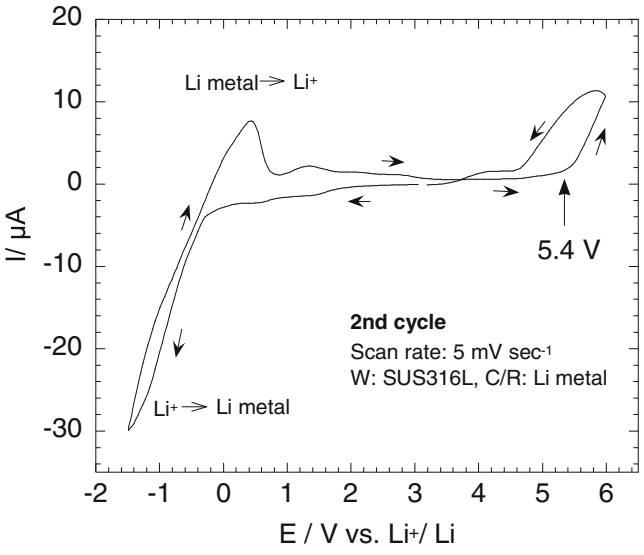

Fig. 11 Cyclic voltammogram of the PDMS-2SiA/LiTFSA complex with a salt concentration of 50 mol% with respect to silatrane units

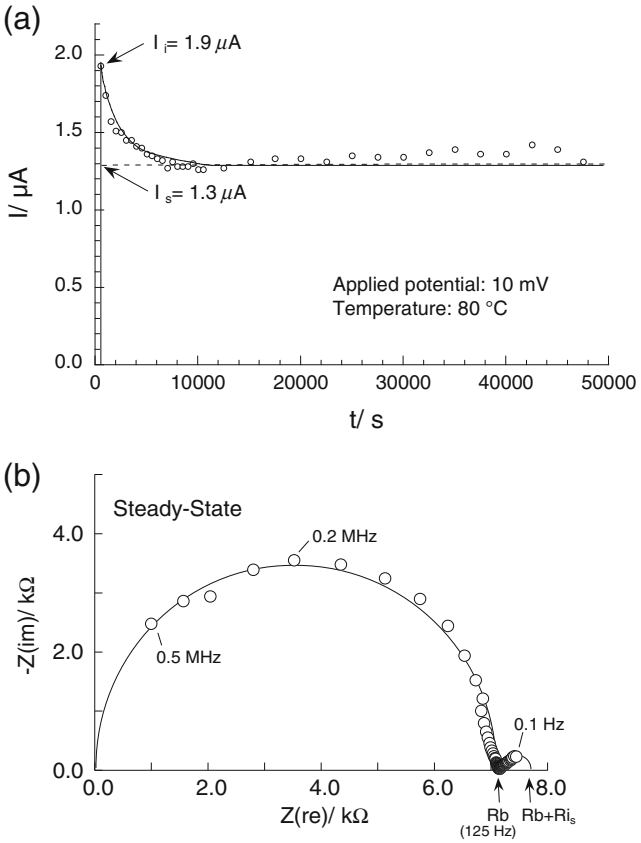

Fig. 12 **a** Time dependent current for the PDMS-2SiA/50 mol% LiTFSA complex in the dc polarization with a bias of 10 mV. **b** Nyquist plot of the PDMS-2SiA/50 mol% LiTFSA complex

$$t_{Li+} = I_s(V - I_i Ri_i)/I_i(V - I_s Ri_s) \quad (2)$$

V denotes the applied potential (10 mV). The relatively high lithium-ion transference number could be attributed to the low Lewis basicity of the PDMS backbone [40], which does not suppress cation mobility. Furthermore, although the Lewis acidity of the silicon in the silatrane moiety is low because of the transannular coordination by the nitrogen, the TFSA anion may competitively interact with the silatrane, thus favoring a higher lithium-ion transport.

4 Conclusions

Polysiloxanes with silatrane units were prepared, which dissolved lithium salts to form a solvent-free lithiumion conductor. Wide potential window (5.4 V), high lithium-ion transference number (0.70), and good thermal durability (at least 150 °C) were attained in the PDMS-2SiA/LiTFSA complex. The relatively low ionic conductivity of 10^{-5} S cm^{-1} at ambient temperature is the drawback of this material though it exceeds 10^{-4} S cm^{-1} above 100 °C. The present polymers might preferably be used as binders for electrode materials or hard-solid electrolyte materials.

Acknowledgments This research was supported by a Grant-in-Aid for Scientific Research (KAKENHI: No. 24750111 and 24102005) from the Japan Society for the Promotion of Science. This research was also supported by JST-CREST. We acknowledge the financial supports from Mitsubishi Rayon, Hiroshima Bank, and Electric Technology Research Foundation of Chugoku.

References

1. Kamaya N, Homma K, Yamakawa Y, Hirayama M, Kanno R, Yonemura M, Kamiyama T, Kato Y, Hama S, Kawamoto K, Mitsui A (2011) A lithium superionic conductor. Nat Mater 10:682–686
2. Tatsumisago M, Hayashi A (2012) Superionic glasses and glass-ceramics in the Li_2S-P_2S_5 system for all-solid-state lithium secondary batteries. Solid State Ionics 225:342–345
3. Yoshida K, Nakamura M, Kazue Y, Tachikawa N, Tsuzuki S, Seki S, Dokko K, Watanabe M (2011) Oxidative-stability enhancement and charge transport mechanism in glyme-lithium salt equimolar complexes. J Am Chem Soc 133:13121–13129
4. Yoshida K, Tsuchiya M, Tachikawa N, Dokko K, Watanabe M (2012) Correlation between battery performance and lithium ion diffusion in glyme-lithium bis(trifluoromethanesulfonyl)amide equimolar complexes. J Electrochem Soc 159:A1005–A1012
5. Rossi RAA, West R (2009) Silicon-containing liquid polymer electrolytes for application in lithium ion batteries. Polym Int 58:267–272
6. Fish D, Khan IM, Smid J (1986) Conductivity of silid complexes of lithium perchlorate with poly{[ω-methoxyhexa (oxyethylene)ethoxy]methylsiloxane}. Makromol Chem Rapid Commun 7:115–120
7. Spindler R, Shriver DF (1988) Investigations of a siloxane-based polymer electrolyte employing ^{13}C, ^{29}Si, ^{7}Li and ^{23}Na solid state NMR spectroscopy. J Am Chem Soc 110:3036–3043
8. Zhou G-B, Khan IM, Smid J (1993) Solvent-free cation-conducting polysiloxane electrolytes with pendant oligo (oxyethylene) and sulfonate groups. Macromolecules 26:2202–2208
9. Siska DP, Shriver DF (2001) Li^+ conductivity of polysiloxane-trifluoromethylsulfonamide polyelectrolytes. Chem Mater 13: 4698–4700
10. Amine K, Wang Q, Vissers DR, Zhang Z, Rossi NAA, West R (2006) Novel silane compounds as electrolyte solvents for Li-ion batteries. Electrochem Commun 8:429–433
11. Walkowiak M, Schroeder G, Gierczyk B, Waszak D, Osińska M (2007) New lithium ion conducting polymer electrolytes based on polysiloxane grafted with Si-tripodand centers. Electrochem Commun 9:1558–1562
12. Doyle M, Fuller TF, Newman J (1994) The importance of the lithium ion transference number in lithium/polymer cells. Electrochim Acta 39:2073–2081
13. Shodai T, Owens BB, Ohtsuka H, Yamaki J-I. (1994) Thermal stability of the polymer electrolyte $(PEO)_8LiCF_3SO_3$. J Electrochem Soc 141:2978–2981
14. Zhu Z, Einset AG, Yang C-Y, Chen W-X, Wnek GE (1994) Synthesis of polysiloxanes bearing cyclic carbonate side chains. Dielectric properties and ionic conductivities of lithium triflate complexes. Macromolecules 27:4076–4079
15. Lee IJ, Song GS, Lee WS, Suh DH (2003) A new class of solid polymer electrolyte: synthesis and ionic conductivity of novel polysiloxane containing allyl cyanide groups. J Power Sources 114:320–329
16. Zhang Z, Lyons LJ, West R, Amine K, West R (2005) Synthesis and ionic conductivity of mixed substituted polysiloxanes with oligoethyleneoxy and cyclic carbonated substituents. Silicon Chemistry 3:259–266
17. Rossi NAA, Wang Q, Amine K, West R (2010) Silicon-containing cabonates- Synthesis, characterization, and additive effects for silicon-based polymer electrolytes. Silicon 2:201–208
18. Liang S, Choi UH, Liu W, Runt J, Colby RH (2012) Synthesis and lithium ion conduction of polysiloxane single-ion conductors containing novel weak-binding borates. Chem Mater 24:2316–2323
19. Mizumo T, Fujita R, Ohshita J (2011) Lithium ion conduction in silatrane matrices. Chem Lett 40:798–800
20. Frye CL, Vogel GE, Hall JA (1961) Triptych-siloxazolidines: pentacoordinate bridgehead silanes resulting from transannular interaction of nitrogen and silicon. J Am Chem Soc 83:996–997
21. Frye CL, Vincent GA, Finzel WA (1971) Pentacoordinate silicon compounds. V. Novel silatrane chemistry. J Am Chem Soc 93:6805–6811
22. Voronkov MG, Dyakov VM, Kirpichenko SV (1982) Silatranes. J Organomet Chem 233:1–147
23. Puri JK, Singh R, Chahal VK (2011) Silatranes: a review on their synthesis, structure, reactivity and applications. Chem Soc Rev 40:1791–1840
24. Laine RM, Treadwell DR, Mueller BL, Bickmore CR, Waldner KF, Hinklin TR (1996) Processable aluminosilicate alkoxide precursors from metal oxides and hydroxides. The oxide one-pot synthesis process. Mater Chem Commun 6:1441–1443
25. Cheng H, Laine RM (1999) Simple, low-cost synthetic route to potentially polymerizable silatranes. New J Chem 23:1181–1186
26. Armand MB, Bruce PG, Forsyth M, Scrosati B, Wieczorek W (2011) Polymer electrolytes In: Bruce DW, O'Hare D, Walton RI (eds) Energy materials, Wiley, Chichester pp 1–31
27. Mizumo T, Kajihara T, Yamada T, Ohshita J (2013) Preparation and utilization of poly(methacryloylsilatrane) as a salt-dissociation enhancer in PEO-based polymer electrolytes. Polym Adv Technol 24:705–714
28. Evans J, Vincent CA, Bruce PG (1987) Electrochemical measurement of transference numbers in polymer electrolytes. Polymer 28:2324–2328
29. Egorov YP, Voronkov MG, Lutsenko TB, Zelchan GI (1966) Infrared absorption spectra of silatranes. Khim Geterotsikl Soedin 2:24–33

30. Cai D, Neyer A, Kuckuk R, Heise HM (2010) Raman, mid-infrared, near-infrared and ultraviolet-visible spectroscopy of PDMS silicone rubber for characterization of polymer optical waveguide materials. J Mol Struct 976:274–281
31. Smith BC (1998) Infrared spectral interpretation. CRC Press, Boca Raton
32. Imura K (2012) Non-aqueous electrolytes containing fluorine. Molten Salts 55:99–102
33. Barthel J, Gores HJ, Neueder R, Schmid A (1999) Electrolyte solutions for technology-new aspects and approaches. Pure Appl Chem 71:1705–1715
34. Markusson H, Johansson P, Jacobsson P (2005) Electrochemical stability and lithium ion-anion interactions of orthoborate anions (BOB, MOB, BMB), and presentation of novel anion: tris-oxalato-phosphate. Electrochem Solid-State Lett 8:A215–A218
35. Johansson P, Jacobsson P (2001) New lithium salts on the computer: fiction or fact? Electrochim Acta 46:1545–1552
36. Torell LM, Jacobsson P, Sidebottom D, Petersen G (1992) The importance of ion-polymer crosslinks in polymer electrolytes. Solid State Ionics 53–56:1037–1043
37. Sylla S, Sanchez JY, Armand M (1992) Electrochemical study of linear and crosslinked POE-based polymer electrolytes. Electrochim Acta 37:1699–1701
38. Ohno H (2008) Physical properties of ionic liquids for electrochemical applications In: Endres F, Abbott AP, MacFarlane DR (eds) Electrodeposition from ionic liquids, Wiley, Weinheim, pp 47–82
39. Takekawa T (2010) Approach and task of ionic liquid electrolyte for fuel cell under high temperature and non-humidification. Molten Salts 53:110–114
40. West R, Whatley LS, Lake KJ (1961) Hydrogen bonding studies. V. The relative basicities of ethers, alkoxysilanes and siloxanes and the nature of the silicon-oxygen bond. J Am Chem Soc 83:761–764